Semiflexible Filamentous Composites

E. M. Huisman,[1] C. Heussinger,[2] C. Storm,[3] and G. T. Barkema[1,4]

[1]*Universiteit Leiden, Instituut-Lorentz, Postbus 9506, NL-2300 RA Leiden, The Netherlands*
[2]*Université de Lyon; Université Lyon I, Laboratoire de Physique de la Matière Condensée et Nanostructures; UMR CNRS 5586, 69622 Villeurbanne, France*
[3]*Department of Applied Physics and Institute for Complex Molecular Systems, Eindhoven University of Technology, P.O. Box 513, NL-5600 MB Eindhoven, The Netherlands*
[4]*Universiteit Utrecht, Institute for Theoretical Physics, NL-3584 CE Utrecht, The Netherlands*

(Received 31 May 2010; published 8 September 2010)

Inspired by the ubiquity of composite filamentous networks in nature, we investigate models of biopolymer networks that consist of interconnected floppy and stiff filaments. Numerical simulations carried out in three dimensions allow us to explore the microscopic partitioning of stresses and strains between the stiff and floppy fractions c_s and c_f and reveal a nontrivial relationship between the mechanical behavior and the relative fraction of stiff polymer: when there are few stiff polymers, nonpercolated stiff ''inclusions'' are protected from large deformations by an encompassing floppy matrix, while at higher fractions of stiff material the stiff network is independently percolated and dominates the mechanical response.

DOI: 10.1103/PhysRevLett.105.118101 PACS numbers: 87.19.rd, 62.25.−g, 87.16.af

The basic design of most structural biological materials is that of a cross-linked meshwork of semiflexible protein polymers. The mechanical properties of these biomaterials are biologically highly significant [1,2]. Understanding these properties at the bulk or continuous level is not sufficient: biological entities such as cells, motor proteins, and sensory complexes experience, manipulate, and interact with these polymer networks at single-filament length scales and are therefore intimately aware of the discrete nature of these materials. Another complication arises when considering that most structural biomaterials are in fact composites: bidisperse or polydisperse mixtures of different protein polymers. The extracellular matrix consists of a mixture of stiff collagen and flexible elastin filament (bundles), and the relative abundance of these two greatly affects mechanical properties [3]. A more specific example that derives much of its biological function from the side-by-side deployment of mechanically vastly different filaments is articular cartilage—a complex, partially ordered composite containing type-II collagen and proteoglycans as its main structural components [4]. Composite physics may be at play in single-component networks: coexistent and interlinked single fibers and fiber bundles determine the mechanical properties of actin gels and actin-filamin networks [5]. The interplay between stiff and floppy elements goes far beyond simple property mixing, as demonstrated by yet another striking example of a composite network: the cytoskeleton. The network of relatively floppy filamentous actin (F-actin) and intermediate filaments is believed to be nonlinearly stiffened by the rigid microtubules, and experiments have hinted at significant tensional forces in the cellular actin [6,7]. The cell cytoskeleton, which is built up from microtubules, actin filaments, and intermediate filaments, is yet another striking example of a composite network.

Significant effort has been devoted to model systems of homogeneous and isotropic *single-component* networks of biopolymers, such as F-actin and collagen [8–16]. The single filaments that constitute these networks can be described by the semiflexible wormlike chain force-extension curve, where extension requires that thermal fluctuations of the filaments be suppressed leading to a steep and nonlinear increase in the force. Compression requires considerably smaller forces that become constant in the Euler buckling limit [8,9]. Networks of such filaments show highly nonlinear strain stiffening and negative normal forces under shear [10,11]. Recent theoretical studies and simulations have also underlined the importance of nonaffine bending deformations in these networks [12,14–16]. Models applying a similar method to composite biomaterials have only recently begun to emerge [17,18] and have focused on bulk behavior.

In this Letter, we report the results of a series of numerical experiments of *two-component* networks of biopolymers to determine the relationship between composition and mechanical properties, both on the single filament as well as on the bulk level. Furthermore, we compare our results to a theoretical model.

Our networks consist of long filaments that are permanently cross-linked. These cross-links force a binary bond between two filaments, without angular preferences. The filaments are described by the semiflexible wormlike chain model [8,9]. The degrees of freedom of the segments (parts of filaments in between two cross-links) are integrated out to obtain an effective Hamiltonian. This effective Hamiltonian gives the energy for each network

configuration, characterized by the network topology, the positions of the cross-links, and the link-to-link separation of the filaments between cross-links. Starting from a random, isotropic network consisting of cross-links and segments, we apply a large number of Monte Carlo moves which alter the network topology such that filaments with a persistent directionality along segments are formed. At this point, we designate filaments to be either stiff or floppy by assigning to each segment a persistence length and an equilibrium backbone length. We then further relax the configuration by applying new Monte Carlo moves. All our networks have periodic boundary conditions and contain 1000 cross-links. Their lateral sizes are determined by the condition of zero pressure. A detailed description of this approach is presented in [14]. Our networks are characterized by the following set of parameters: the persistence length ℓ_p of the stiff filaments, the stiffness ratio $R_p = \ell_p/\ell_{p,\text{floppy}}$, the average filament length L, the average distance between cross-links along a polymer's backbone ℓ_c, and finally the relative fraction of stiff filaments c_s. In this work, we examine the c_s dependence of the mechanical behavior. We restrict ourselves to a biologically relevant region of parameter space: the persistence length $\ell_{p,\text{floppy}}$ of the floppy filaments and the cross-link distance ℓ_c are of comparable magnitude. On average, each filament is cross-linked 6 times ($L = 6l_c$). The ratio of the persistence lengths of stiff and floppy filaments R_p is chosen to be 16 or 64. While this ratio is smaller than that for collagen and elastin composites ($R_p \approx 100$) [3], or microtubule and F-actin composites ($R_p > 200$) [19], it is large enough to capture the qualitative behavior of such composite networks. Unless otherwise stated, all data shown represent the averages of nine network realizations.

Our key findings are summarized in Fig. 1. In Fig. 1(a) we plot a 50/50 composite: rather than averaged, the mechanical behavior is bimodal—approaching the fully floppy system at low strains but, at finite strains, resembling the fully stiff network. We stress that this type of response can only be achieved in a composite. Even the linear behavior does not interpolate simply between stiff and floppy: Fig. 1(b) shows that at low to intermediate c_s, the modulus is quite insensitive to c_s, but rises very quickly at higher c_s. Figure 1(c), finally, reinforces the point of Fig. 1(a): although the effects of adding stiff polymer are hardly noticeable in the linear elastic behavior, their effect on the nonlinear behavior is felt much earlier. The critical strain (γ_c) for the onset of the nonlinear regime reacts immediately to the addition of stiff material, but saturates at a point roughly coincident with the rise of the linear modulus.

The qualitative picture that emerges at small c_s is one of a floppy matrix encompassing isolated stiff filaments, or nonpercolated clusters. Intuitively, the initial insensitivity of the linear modulus K_0 to the addition of stiff material makes sense: deforming the stiff filaments requires higher energies than deforming the softer elements, and therefore the low-energy modes of the system favor straining the floppy elements over the stiff ones. As long as stiff filaments do not form an independently load-bearing subnetwork, these low-energy modes exist and are compatible with the bulk deformation.

This interpretation is confirmed by an examination of the microscopic deformation field, characterized by the nonaffinity parameter $A = \langle|\mathbf{x}_{\text{aff}} - \mathbf{x}|^2\rangle/\gamma^2$ [Fig. 2(a)]. This parameter quantifies the deviation of the local deformations, $\mathbf{x}$, from a homogeneous affine deformation field, $\mathbf{x}_{\text{aff}}$. As shown in previous numerical work [16] and in experiments [20], the nonaffinity generally increases with increased stiffness of the filaments, as bending deformations are more important for the network response of stiffer filaments. Indeed we find that the nonaffinity is minimal

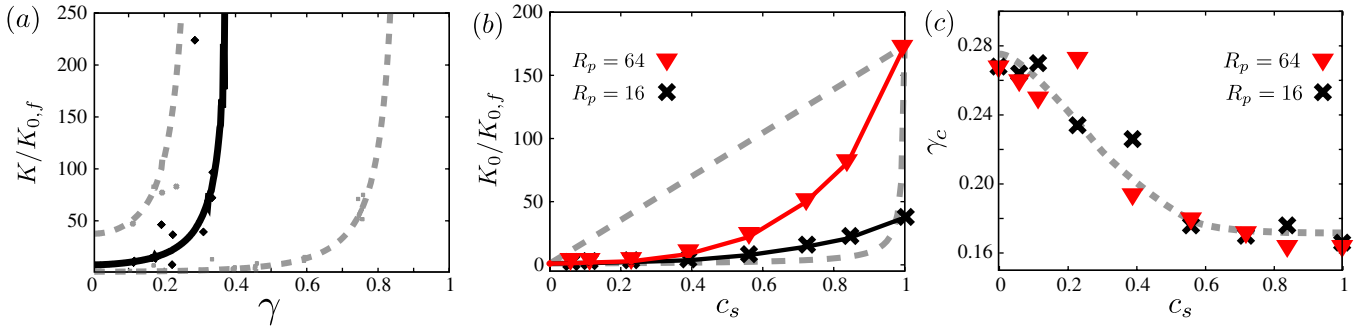

FIG. 1 (color online). Macroscopic properties of the networks as a function of the fraction c_s of stiff filaments in a network. (a) Shear modulus K as a function of shear γ, normalized by the initial shear modulus $K_{0,f}$ of single-component networks of floppy filaments. The different curves represent the stiffness of networks with $c_s = 0.0, 0.56, 1.0$ (from bottom to top), at a fixed persistence length ratio $R_p = 16$. Some data points (<1%) lie well outside the curve; these are indicated by the symbols. These outliers occur due to local reorientations, cf. [14]. (b) The normalized initial shear modulus as a function of c_s, for networks with $R_p = 64$ and 16. For comparison, we also plot curves corresponding to a linear scaling of the shear modulus with c_s, given by $K_0(c_s) = c_s K_{0,s} + (1 - c_s)K_{0,f}$, and a linear scaling of the compliance with c_s, given by $1/K_0(c_s) = c_s/K_{0,s} + (1 - c_s)/K_{0,f}$. (c) Critical shear γ_c, defined as the shear at which the shear modulus is twice the initial shear modulus, as a function of c_s. The curve is drawn as a guide to the eye.

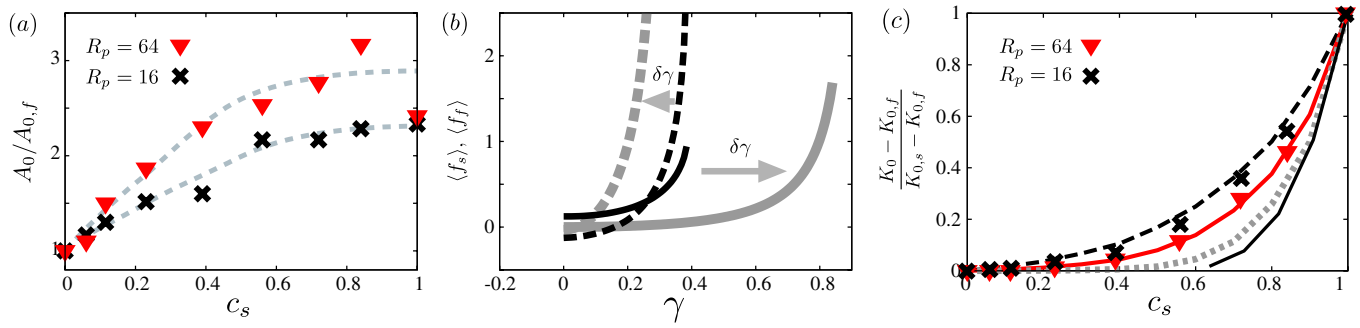

FIG. 2 (color online). (a) The nonaffinity at zero shear divided by the initial nonaffinity of a network with $c_s = 0$. The curves are drawn as guides to the eye. (b) Average forces in the floppy and stiff filaments during deformation, shown by the solid and dotted curves, respectively. The black curves represent the average force of a network with $c_s = 0.56$ during shear. For comparison, we plot the average forces in single-component networks, $c_s = 1.0$ and $c_s = 0.0$ (gray curves). As indicated by the arrows, the curves for the average forces in the composite networks are shifted along γ with respect to the curves for the single-component network. (c) The scaled initial stiffness as a function of c_s, obtained by the floppy-mode model for $R_p = 16, 64, 1000, \infty$ (from top to bottom). For comparison, the data from simulations are given by the symbols.

for purely floppy networks and rises roughly linearly with the addition of stiff material. Such a linear increase represents the generic behavior of low-density (stiff) inclusions that independently perturb the deformation field of their surrounding (floppy) matrix [21]. These additional nonaffine deformations bring the floppy filaments closer to the nonlinear part of their force-extension relation, giving rise to the decrease of the critical strain γ_c as displayed in Fig. 1(c).

In the nonlinear regime the inherent stiffening of a single semiflexible polymer makes the distinction between floppy and stiff fractions highly strain dependent, with the ratio of their nonlinear moduli tending to unity in the high strain limit. This suggests a self-matching behavior at finite strain: the floppy network stiffens up to the point where its modulus matches that of the stiff network. Beyond this point, the entire meshwork behaves as a nearly monodisperse system of stiff filaments. This effect is the origin of the behavior in Fig. 1(a): at high strains, the entire system is ultimately forced to couple to the stiffer deformation modes.

This mechanism of stiffness matching is further illustrated in Fig. 2(b), which shows the average forces in the stiff and floppy filaments during deformation. By comparing with the one-component networks (gray lines), we can define a strain shift $\delta\gamma$: For given network strain γ, the filaments in the composite behave as if they were strained up to $\gamma + \delta\gamma$. Apparently, the effective strain on the floppy filaments is much larger than that on the stiff filaments. Equivalently, high forces in stiff filaments are suppressed, at the cost of increased forces in floppy filaments.

Interestingly, this load partitioning persists even at *zero strain*, where stiff filaments are, on average, compressed while floppy filaments are stretched out. This simultaneously stretched and compressed ground state is tantalizingly reminiscent of tensegrity states [7]. Apparently, dense cross-linking restricts relaxation of the network, and the absolute minimum of mechanical energy cannot be attained. There is, therefore, always a finite amount of residual elastic energy. This suggests that such force distributions may not be a deliberate design principle but rather are the necessary by-product of polydispersity in filamentous composites.

The picture of a floppy matrix embedding stiffer inclusions breaks down when the stiff filaments become independently rigidity percolated: the point where deformation of the stiff elements becomes inevitable. We may estimate the percolation threshold by a counting argument [22]. Equating the number of degrees of freedom of the stiff filaments to the number of constraints due to cross-links between stiff filaments gives (for $L/\ell_c = 6$) a threshold $c_s = 0.56$. This marks the transition from the low to the high c_s regime and coincides roughly with the rise in the linear modulus K_0 [Fig. 1(b)]. Two separate observations confirm the onset of stiff dominance: First, $c_s = 0.56$ is the point at which the nonaffinity, which we attribute to the floppy matrix attempting to work around the stiff fraction, begins to plateau at the level of the bending dominated response of a purely stiff network. Second, the critical strain γ_c levels off around this same value of c_s. In the range of stiffness ratios (R_p) accessible to the simulations, the percolation is rather "soft" and represents a smooth crossover phenomenon. The approach towards the singular percolation limit, $R_p = \infty$, has, for example, been studied in simulations of mixed random resistor networks [23]. To address the analogous problem we compare our results with theoretical considerations, in which the parameter R_p can be tuned to arbitrarily large values. The "floppy-mode" theory [12] has recently been shown to capture quite well the elasticity in one-component isotropic [24,25] as well as anisotropic networks [26]. Within this theoretical framework the calculation of the network elastic modulus is reduced to the description of a "test" filament in an array of pinning sites. The coupling strength to these sites, k, represents the elastic modulus of the network and has to be

calculated self-consistently. To generalize this model to the case of composite networks, we use two different test chains with coupling parameters k_f and k_s, representing floppy and stiff filaments, respectively [27]. The use of two different coupling strengths quite naturally takes into account the load partitioning encountered in the simulations. The network modulus, $k = c_s k_s + (1 - c_s)k_f$, is obtained by solving the two equations

$$k_{f/s} \simeq \left\langle \min_y \left(W_b^{f/s}[y(s)] + \frac{1}{2} \sum_{i=1}^{n} k_{\alpha_i} (y(s_i) - \bar{y}_i)^2 \right) \right\rangle, \quad (1)$$

where $k_{\alpha_i} = k_s, k_f$ with probability c_s and $1 - c_s$, respectively. The two energy contributions on the right-hand side of Eq. (1) reflect the competition between the bending energy of the (floppy or stiff) filament, $W_b^{f/s}$, and the energy due to deformation of the surrounding medium by displacing the pinning sites (located at arclength position s_i along the filament). The nonlinear entropic stretching elasticity is not included in these equations. The minimization is to be performed over the contour of the filament, $y(s)$, the angular brackets specify the disorder average over the network structure.

Figure 2(c) displays the results from this calculation for various stiffness ratios R_p, showing a sharp percolation transition in the limit $R_p \to \infty$. The model compares well with the simulation data, even though the stretching elasticity is not accounted for. This indicates that the bending stiffness is likely the dominant factor in determining the rise of the linear elastic modulus, in agreement with the proposed mechanism of load partitioning and the observed increase of the nonaffinity.

In conclusion, our results demonstrate that the mechanical behavior of filamentous composites is considerably richer than the simple proportional mixing of properties. The fact that the floppy and stiff networks are physically linked causes a strongly nonlinear coupling between the strain fields which deeply affects composite mechanics. This may explain the ubiquity of composites in structural biological applications: slight variations in composition cause large changes in mechanical behavior. This high susceptibility makes the composite architecture an attractive motif for biological regulation. Likewise, the ''best of both worlds'' aspect may be exploited by nature: composites combine the initial softness of their most compliant components with the ultimate toughness of the stiffest elements. This greatly enhances the stiffness range of nonlinearly elastic materials. Moreover, composites do so in a manner that could never be attained in monodisperse materials, since linear and nonlinear properties of composites are determined by two physically different materials and therefore may be independently varied. This possibility of independently tuning the linear and nonlinear behavior also has considerable potential for the design of biomimetic or bioinspired synthetic materials and deserves further exploration.

It is a pleasure to thank Paul Janmey for helpful discussions. C. S. and C. H. acknowledge the hospitality of the Aspen Center for Physics where part of this work was carried out. C. H. thanks the von Humboldt foundation for financial support.

[1] A. R. Bausch and K. Kroy, Nature Phys. **2**, 231 (2006).
[2] P. A. Janmey and D. A. Weitz, Trends Biochem. Sci. **29**, 364 (2004).
[3] L. D. Black *et al.*, Biophys. J. **94**, 1916 (2008).
[4] P. Bullough and J. Goodfellow, J. Bone Jt. Surg. **50**, 852 (1968).
[5] K. M. Schmoller, O. Lieleg, and A. R. Bausch, Phys. Rev. Lett. **101**, 118102 (2008); K. M. Schmoller, O. Lieleg, and A. R. Bausch, Soft Matter **4**, 2365 (2008).
[6] J. Mizushima-Sugano, T. Maeda, and T. Miki-Noumura, Biochim. Biophys. Acta **755**, 257 (1983).
[7] D. E. Ingber, J. Cell Sci. **116**, 1157 (2003).
[8] F. C. MacKintosh, J. Käs, and P. A. Janmey, Phys. Rev. Lett. **75**, 4425 (1995).
[9] C. Storm *et al.*, Nature (London) **435**, 191 (2005).
[10] P. A. Janmey *et al.*, Nature (London) **345**, 89 (1990).
[11] P. A. Janmey *et al.*, Nature Mater. **6**, 48 (2007).
[12] C. Heussinger, B. Schaefer, and E. Frey, Phys. Rev. E **76**, 031906 (2007).
[13] J. A. Åström *et al.*, Phys. Rev. E **61**, 5550 (2000).
[14] E. M. Huisman, C. Storm, and G. T. Barkema, Phys. Rev. E **78**, 051801 (2008).
[15] P. R. Onck *et al.*, Phys. Rev. Lett. **95**, 178102 (2005)
[16] E. M. Huisman *et al.*, Phys. Rev. Lett. **99**, 208103 (2007).
[17] C. P. Broedersz, C. Storm, and F. C. MacKintosh, Phys. Rev. Lett. **101**, 118103 (2008).
[18] H. Wada and Y. Tanaka, Europhys. Lett. **87**, 58 001 (2009).
[19] F. B. Gittes *et al.*, J. Cell Biol. **120**, 923 (1993).
[20] Q. Wen *et al.*, New J. Phys. **9**, 428 (2007).
[21] S. Torquato, *Random Heterogeneous Materials* (Springer, New York, 2002).
[22] J. C. Maxwell, Philos. Mag. **27**, 294 (1864).
[23] J. P. Straley, Phys. Rev. B **15**, 5733 (1977).
[24] O. Lieleg *et al.*, Phys. Rev. Lett. **99**, 088102 (2007).
[25] C. Heussinger and E. Frey, Phys. Rev. Lett. **97**, 105501 (2006); Eur. Phys. J. E **24**, 47 (2007).
[26] A. R. Missel *et al.*, arXiv:1002.4440.
[27] Details of the calculation will be published elsewhere.